Proton transfer in hydrogen-bonded crystalline KH_2PO_4

1996 J. Phys.: Condens. Matter 8 603

(http://iopscience.iop.org/0953-8984/8/5/010)

J. Phys.: Condens. Matter **8** (1996) 603–618. Printed in the UK

Proton transfer in hydrogen-bonded crystalline KH_2PO_4

Hidehiko Sugimoto† and Susumu Ikeda‡

† Department of Physics, Faculty of Science and Engineering, Chuo University, Kasuga, Bunkyo-ku, Tokyo 112, Japan

‡ National Laboratory for High Energy Physics, Oho 1-1, Tsukuba, Ibaraki 305, Japan

Received 21 June 1995, in final form 18 September 1995

Abstract. Properties of the proton transfer in KH_2PO_4 (KDP) are examined on the basis of a model that was proposed to explain the mechanism of the phase transition from a ferroelectric phase to a paraelectric phase; it is found that, in the paraelectric phase, a proton transfers from one site to the other site at a jump rate of the order of 10^{12} s^{-1}.

Scattering functions for incoherent scattering of thermal neutrons induced by the proton motion are also calculated in the framework of the classical approximation.

1. Introduction

Most of the theoretical studies [1–6] concerning properties of hydrogen-bonded materials with the ferroelectric (antiferroelectric) phase transition like KH_2PO_4 (KDP) are based on the assumption introduced by Slater [7] and refined by Takagi [8]: the static and dynamic properties of these systems are described on the basis of the configuration energy determined by proton configurations. Recent experiments, however, have revealed that the phase transition of this type exists even in materials in which the hydrogen-bond network is closed in a dimer—for example, $K_3D(SO_4)_2$ [9, 10]. This seems to indicate that studies from different points of view are required to explain properties of hydrogen-bonded materials including the mechanism of the phase transition.

One such study has been performed by Kojyo and Onodera [11] recently. They proposed a dipole–proton model in which a strong coupling between protons and dipole moments is assumed, and showed that properties of the ferroelectric phase transition in CsH_2PO_4 are explained by this model.

One of the striking features of the phase transition in hydrogen-bonded materials is that there is a large isotope effect on the transition temperature T_c. For example, KDP and its deuterated isomorph KD_2PO_4 (DKDP) undergo phase transitions at 122 and 213 K, respectively. To explain such remarkable isotope effects, the tunnelling motion of protons proposed by Blinc [12] and by Tokunaga and Matsubara [13] has been introduced for both cases—the Slater–Takagi model and the dipole–proton model. Although the introduction of the tunnelling motion gives an explanation for the large isotope effect on the transition temperature, at present there is no observation of direct evidence for the tunnelling motion of protons (deuterons), in spite of recent careful experiments [14, 15]. Furthermore, Ichikawa [16] found that, in KDP, the increase in T_c upon deuteration may be attributed to an accompanying increase in the oxygen–hydrogen–oxygen bond (O–O bond) distance, d. Later, Nelmes [18] re-examined the high-resolution neutron diffraction results for KDP and DKDP, and confirmed that this geometric isotope effect plays an important role for the

0953-8984/96/050603+16$19.50

increase in T_c upon deuteration although part of the increase is caused by a direct tunnelling effect.

Recently, we proposed a new model for the mechanism of the phase transition in KDP [18], based on the dipole–proton model proposed by Kojyo and Onodera, but not introducing the tunnelling motion of protons explicitly. From the examination of this model [18, 19], we found the following features: (1) the phase transition is of order–disorder type with a large isotope effect on the transition temperature, in agreement with experiments; (2) the isotope effect is due to changes of shape of the potential acting on a proton, induced by ordering of the dipole moments, but not the tunnelling motion of protons; (3) a change in d makes an important contribution to a change in T_c, in addition to the effect of mass; (4) the excitation energies for the proton motion in the direction along an O–O bond are distributed over a wide energy region. These features agree with those of observations for KDP [14, 20–23].

In our previous paper [24] (from now on referred to as I), furthermore, the motion of dipole moments was examined in the framework of the harmonic approximation; it was shown that, in the ferroelectric phase, there are electric dipole waves, via which the vibration motion of protons is induced along the direction of O–O bonds. This motion of protons is expected to be detected by neutron scattering experiments. In fact, Shibata and Ikeda [23] found a peak at 28 meV in energy spectra obtained from incoherent inelastic neutron scattering, in addition to peaks corresponding to the excitation of protons to excited states. Our conclusion was that the observed peak at 28 meV is to be regarded as a peak due to the vibration motion of protons induced by the electric dipole wave.

In this paper, we examine the motion of dipole moments in our model numerically. On the basis of the results, dynamic properties of protons in the paraelectric phase are discussed. Our plan is as follows. In section 2, the main features of our model are described. We emphasize here that the proton transfer is caused by the adiabatic transition. Calculations using the Langevin formulation are performed to examine the motion of dipole moments and some results obtained are mentioned in section 3. In section 4, we discuss properties of scattering functions of the incoherent neutron scattering induced by the motion of protons. Finally, in section 5, some aspects of our results are discussed, including a comparison between scattering functions obtained and those of a recent experiment.

The purpose of the present paper is to clarify dynamic properties of protons in KDP, based on our model.

2. Model

2.1. The dipole–proton system

We consider a system comprising N distorted PO_4 tetrahedra and $2N$ protons, under the assumption that (1) the distortion of tetrahedron i is proportional to its electric dipole moment μ_i; and (2) all dipole moments of the tetrahedra lie along the c axis in a KDP crystal. We write the Hamiltonian for this system as follows:

$$H = H_p + H_{p-d} + H_d. \tag{1}$$

Here, H_p is the Hamiltonian for protons, defined by

$$H_p = \sum_{\alpha=1}^{2N} \left(\frac{p_\alpha^2}{2m} + U_\alpha \right) \tag{2}$$

where m is the proton mass, and p_α the momentum of proton α. U_α is a potential acting on the proton, which has double minima on the O–O bond. The interaction energy between protons and dipole moments, H_{p-d}, is assumed to be expressed as

$$H_{p-d} = -\sum_{\alpha=1}^{2N} K(\mu_i + \mu_j)x_\alpha \tag{3}$$

where μ_i and μ_j, respectively, are dipole moments of two tetrahedra (i and j) connected by proton α, x_α is the position of the proton measured from the centre of the O–O bond, and K is a coupling constant. The Hamiltonian for dipole moments, H_d, is as follows:

$$H_d = -\sum_i \frac{\hbar^2}{2M}\frac{\partial^2}{\partial \mu_i^2} + \sum_i \frac{A}{2}\mu_i^2 + \sum_{i,j} D_{i,j}\mu_i\mu_j. \tag{4}$$

Here, M in the first term is an effective mass of a dipole moment, the second term is the elastic energy due to deformation of the tetrahedra, and the third term is the energy of interaction between dipoles.

Protons are expected to follow the motion of dipole moments because of the smallness of proton mass. The adiabatic approximation that separates the motion of fast protons from that of slow dipole moments should, therefore, be valid for the description of the present system. In this approximation, the wave function of the system is written as

$$\Psi(\boldsymbol{r}_1, \cdot\cdot, \boldsymbol{r}_{2N}, \mu_1, \cdot\cdot, \mu_N) = \chi(\{\mu_i\}) \prod_{\alpha=1}^{2N} \psi(\boldsymbol{r}_\alpha; \{\mu_i\}) \tag{5}$$

where $\chi(\{\mu_i\})$ is the wave function of the dipole moments and $\psi(\boldsymbol{r}_\alpha; \{\mu_i\})$ the ground-state wave function of proton α.

The adiabatic potential of the system may be expressed as a function of N dipole moments. We write it as [18, 19, 24]

$$E_{pot} = \frac{A}{2}\sum_{i=1}^{N}\mu_i^2 + \frac{B}{4}\sum_{\langle ij\rangle}^{2N}\mu_i\mu_j - \sum_{\langle ij\rangle}^{2N} E_{ij}^0. \tag{6}$$

Here, the first term is the elastic energy due to mechanical deformations of the tetrahedra; the second term is the interaction energy between dipoles that is taking account of only the nearest-neighbour interaction for simplicity; and the last term is the energy of $2N$ protons, where $-E_{ij}^0$ is the ground-state energy of a proton connecting two neighbouring tetrahedra (i and j).

Knowledge of $-E_{ij}^0$ and $\psi(\boldsymbol{r}_\alpha; \{\mu_j\})$ is obtained from quantum mechanical calculations for protons in KDP. In our previous letter [17], we found by using an empirical potential for U_α that the interaction between a proton and dipole moments induces a drastic change of the potential acting on the proton; accordingly, the energy and wave function of the ground state for the proton strongly depend on a sum of dipole moments of two tetrahedra (i and j) connected by the proton, $\mu_i + \mu_j$.

The ground-state energy obtained can be expressed as

$$E_{ij}^0 = [h^2 + I^2K^2(\mu_i + \mu_j)^2]^{1/2} - h \tag{7}$$

using two parameters, h and I [18]. By using equations (6) and (7), it is easy to show that a state in which $\mu_i = \mu_s$ holds for all tetrahedra becomes stable at $T = 0$ K when $A > B$, where μ_s is a saturated dipole moment determined by the condition $\partial E_{pot}/\partial \mu_s = 0$ (see [18, 19]).

In figure 1(a) we show schematically profiles of the ground-state wave function of a proton. When $|\mu_i + \mu_j|$ is large, the wave function of the ground state is strongly localized;

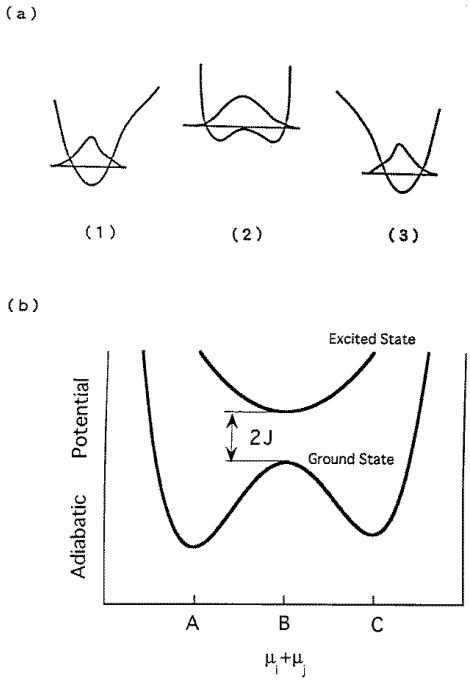

Figure 1. The elementary jump process: (a) schematic profiles of the potential and wave functions of a proton along the direction of an O–O bond (1) at $\mu_i+\mu_j = 2\mu_s$, (2) at $\mu_i+\mu_j = 0$ and (3) at $\mu_i+\mu_j = -2\mu_s$. (b) The adiabatic potential shown schematically. When the system point is at points A, B and C, the proton is in the states (1), (2) and (3), respectively. For the proton transfer from (1) to (3) to occur, it is required that the system point moves from the well at A to the other well at C as a result of thermal fluctuations.

the maximum of its amplitude is at about 0.18 Å from the centre of the O–O bond for $\mu_i + \mu_j = 2\mu_s$ and -0.18 Å for $\mu_i + \mu_j = -2\mu_s$, respectively. The displacement of the proton from the centre is in good agreement with the experimental result obtained from a neutron diffraction measurement [22]. At $\mu_i + \mu_j = 0$, on the other hand, the ground-state wave function extends over a broad potential well and the maximum of its amplitude is located at the centre.

Figure 1(b) gives schematically the features of the adiabatic potentials, E_{pot}, for the ground and excited states of the proton. We emphasize here that there are two equilibrium positions on the O–O bond and that the proton transfers from one equilibrium position to the other equilibrium position passing through the state at $\mu_i + \mu_j = 0$ as a result of thermal fluctuations.

2.2. Proton transfer due to the adiabatic transition

In the adiabatic approximation, a state of the system is represented by a system point on the adiabatic potential surface for the ground state of protons. Under this approximation, we will examine the proton-transfer process in the temperature region where the motion of the system point is described classically.

The transition from one state with the proton wave function localized on the left-hand side (figure 1(a), (1)) to the other state with one localized on the right-hand side (figure 1(a),

(3)) is induced by the movement of the system point from a left-hand well (A in figure 1(b)) in the adiabatic potential surface to a right-hand well (C) passing through the saddle-point configuration (B). The jump rate of the proton is, therefore, expected to be given by

$$\Gamma = \frac{\omega_0}{2\pi} \exp(-E_a/kT) \tag{8}$$

when $E_a > kT$. Here, E_a is the energy difference between the adiabatic potential at point A and that of B, and kT is the thermal energy.

The transfer mechanism is classified according to the magnitude of the excitation energy of the proton at B, $2J$. When J is larger than the vibration energy of the system point in the wells, $\hbar\omega_d$, the proton follows the motion of dipole moments adiabatically [25–28]. In this case of adiabatical transition, the frequency factor ω_0 is given by $\omega_0 \simeq \omega_d$.

If $J < \hbar\omega_d$, the system point undergoes transitions from the adiabatic potential surface for the ground state of the proton to that of the excited state, as is known from the Landau–Zener theory of transition [25, 26]. In the non-adiabatic limit ($J \ll \hbar\omega_d$), the transfer process is accompanied with tunnelling of the proton at the saddle-point configuration, and its jump frequency has the frequency factor ω_0 proportional to J^2 [29, 30]. We emphasize here that ω_0 in the non-adiabatic limit is suitably smaller than that of the adiabatic transition.

In our system, the saddle-point configuration B is a state for which $\mu_i + \mu_j = 0$. Furthermore, the excitation energy of the proton motion along the direction of an O–O bond becomes minimum at $\mu_i + \mu_j = 0$; its value is about 95 meV [18]. On the other hand, the vibration energy of dipoles is of the order of 30 meV as mentioned in I. Thus the relation $J > \hbar\omega_d$ holds. This means that the proton transfer in KDP should be regarded as an adiabatic transition, but not a non-adiabatic transition.

2.3. Calculations on the motion of dipole moments

Upon applying the classical approximation for the motion of dipole moments, the motion of the system point is represented by the following set of equations:

$$M \frac{\mathrm{d}^2\mu_i}{\mathrm{d}t^2} = -\frac{\partial E_{pot}}{\partial \mu_i} \qquad (i = 1, \ldots, N). \tag{9}$$

In the ferroelectric phase, deviations of dipole moments from the saturated value μ_s are expected to be small. Therefore, the linear approximation is valid and can be used to clarify the behaviour of dipole moments, as shown in I. In the paraelectric phase, however, more rigorous treatments beyond the linear approximation are required because the nonlinearity of the equations becomes important.

We must recall here that only the nearest-neighbour interaction is taken into account for the direct interaction between dipole moments in E_{pot} for simplicity. The long-range part of the direct interaction between dipole moments is expected to induce fluctuations of dipole moments, especially, in the paraelectric phase. We assume that this effect can be expressed in terms of the random force and the friction force: a set of Langevin equations

$$M \frac{\mathrm{d}^2\mu_i}{\mathrm{d}t^2} + \beta \frac{\mathrm{d}\mu_i}{\mathrm{d}t} = -\frac{\partial E_{pot}}{\partial \mu_i} + f_i(t) \qquad (i = 1, \ldots, N), \tag{10}$$

is valid for the description of the motion of dipole moments, instead of equation (9), where $f_i(t)$ and β are the random force and the friction constant, respectively. The behaviour of the random force is determined by the condition

$$\langle f_i(t) f_j(0) \rangle = 2\beta kT \, \delta(t) \tag{11}$$

with the assumption that the distribution of $f_i(t)$ be Gaussian with zero mean. Via this condition for $f_i(t)$, the temperature of the system, T, is kept at a constant value [31].

Calculations were performed on a KDP lattice with N $(= 4000)$ tetrahedra imposing a periodic boundary condition, using the Verlet algorithm [32]. In the calculation, we assumed that the random force acting on a dipole moment holds at a constant value over the time interval Δt $(= t_0/20)$ and that its magnitude is given by

$$\langle f_i^2 \rangle = \beta kT/\Delta t. \tag{12}$$

2.4. Static properties

First, we show the temperature dependence of the thermal average of the potential energy, $\langle E_{pot} \rangle$, for various values of β in figure 2(a). It is clear from this figure that $\langle E_{pot} \rangle$ does not depend on values of β; accordingly there is little influence of the random force on the static properties of the system, including the transition temperature T_c.

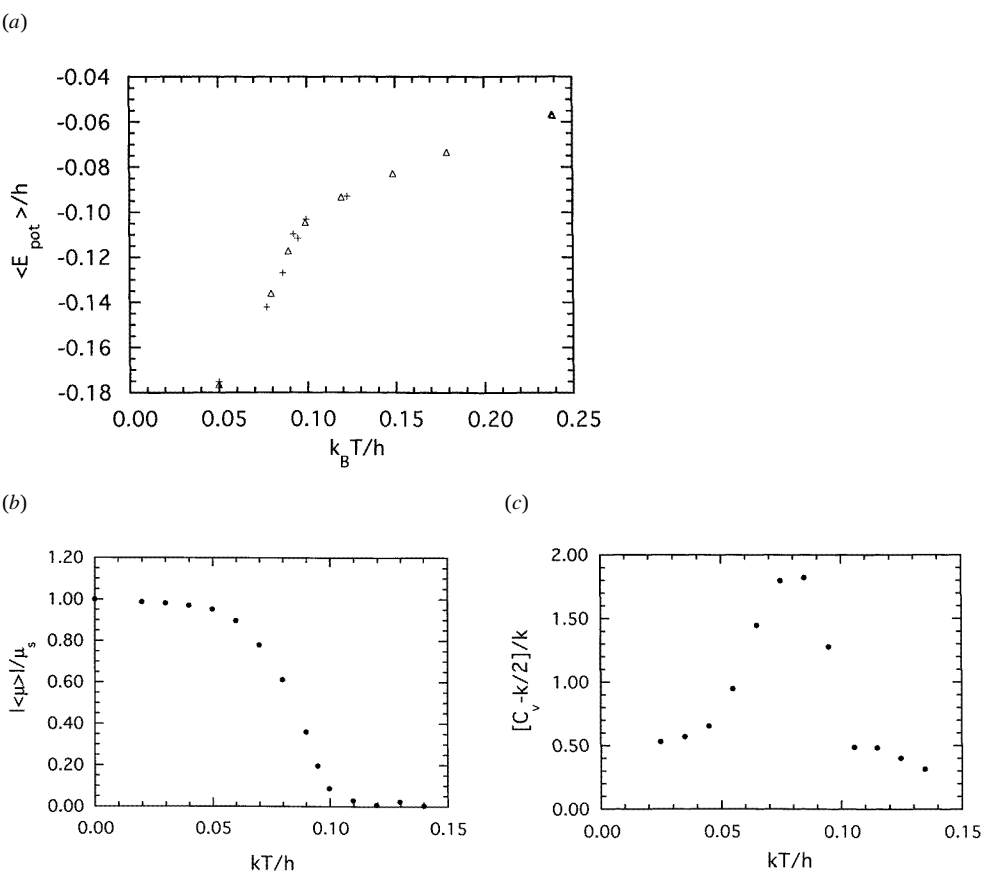

Figure 2. Static properties obtained from the present calculation. Here $\beta_0 = (Mh/\mu_s^2)^{1/2}$. (a) The temperature dependence of the thermal average of the potential energy of the system for various values of β: values for $\beta/\beta_0 = 0$, 0.1 and 0.2 are shown by crosses, and triangles, respectively. (b) The temperature dependence of the thermal average of dipole moments calculated for $\beta/\beta_0 = 0.2$. (c) The specific heat calculated from $\langle E_{pot} \rangle$ for $\beta/\beta_0 = 0.2$.

Figure 2(b) gives the temperature dependence of the thermal average of dipole moments, $\langle\mu\rangle$, calculated by assuming $\beta/\beta_0 = 0.2$. From this figure we can see that there is a phase transition from a ferroelectric phase to a paraelectric phase with $T_c \sim 0.1h/k$ (= 128K).

Figure 2(c) shows the specific heat (c_V) calculated from $\langle E_{pot}\rangle$ for $\beta/\beta_0 = 0.2$ using the relation $c_V = \partial E_{pot}/N\,\partial T + k/2$. We find from this result that there is a peak of c_V at a temperature near to T_c, due to an entropy change induced by the phase transition, and that its transition entropy is about $0.7k$ per tetrahedron.

Table 1. Values of IK, A, B and M used in our calculations for KDP. Here, $h = 0.11$ eV, $\mu_s = 4.8 \times 10^{-22}$ μC cm and $t_0 = 2.0 \times 10^{-14}$ s. The transition temperature, T_c, obtained using these values is also noted.

$IK\mu_s/h$	$A\mu_s^2/h$	$B\mu_s^2/h$	$M\mu_s^2/(ht_0^2)$	T_c (K)
0.6	0.96	0.88	1.0	128

In table 1, the parameters used here are listed with T_c obtained from the present calculation. The static properties obtained here, including the values of T_c, agree well with the previous results obtained from Monte Carlo calculations [19].

2.5. Proton jump rates

Next, we examine dynamic properties of protons. For this, it is important to recall that the mechanism of the proton transfer in our model is regarded as the adiabatic transition, as described in subsection 2.2. In this transition, a change in the sign of a sum of dipole moments of two neighbouring PO_4 tetrahedra, $\mu_i + \mu_j$, means the movement of the system point from one well on the adiabatic potential surface to the other well, in other words, the transfer of the proton connecting the two tetrahedra from one equilibrium position to the other equilibrium position on the O–O bond. Thus we can regard the number of changes in the sign of $\mu_i + \mu_j$ as the number of jumps of the proton between the two sites on the O–O bond, $N(t)$. Under this approximation, therefore, $N(t)$ is evaluated from the time dependence of $\mu_i + \mu_j$. The result is shown in figure 3. As seen in this figure, $N(t)$ is proportional to time; accordingly the jump rate of protons, Γ, is determined from the slope of $N(t)$ in this figure.

The calculated temperature dependence of Γ is shown in figure 4. In the paraelectric phase, Γ shows a weak temperature dependence; its magnitude is comparable with the frequency of the vibration motion of dipole moments. At temperatures below T_c, on the other hand, Γ shows a drastic decrease with decreasing temperature. These features for Γ are hardly altered by changes in the value of β.

To clarify the properties of the proton transfer, we also calculated the probability $W(t)$ that, at time t, the sign of $\mu_i + \mu_j$ remains the same as that at $t = 0$. Results for $W(t)$ at $T = 1.5T_c$ are shown in figure 5.

For the two-site model, in which a proton is assumed to jump between two sites stochastically, $W(t)$ is expressed by

$$W(t) = (1 + \exp(-2\Gamma t))/2. \tag{13}$$

As seen in figure 5, when β is small, $W(t)$ calculated here shows a deviation from this time dependence: it has a broad peak at $t = 3 \times 10^{-13}$ s. This means that the proton transfer is not regarded as a simple Markov process. When β increases, the peak decreases and the

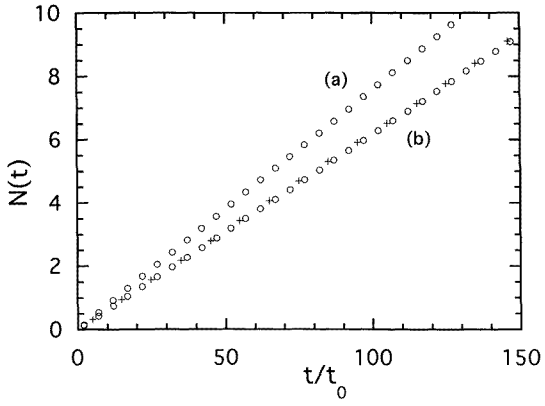

Figure 3. The time dependence of the number of jumps between two sites evaluated from the time dependence of $\mu_i + \mu_j$ at (a) $T = 1.5T_c$ and (b) $T = 2.0T_c$. Results for $\beta/\beta_0 = 0$ and 0.2, respectively, are shown by crosses and circles. Here, $t_0 = 2.0 \times 10^{-14}$ s.

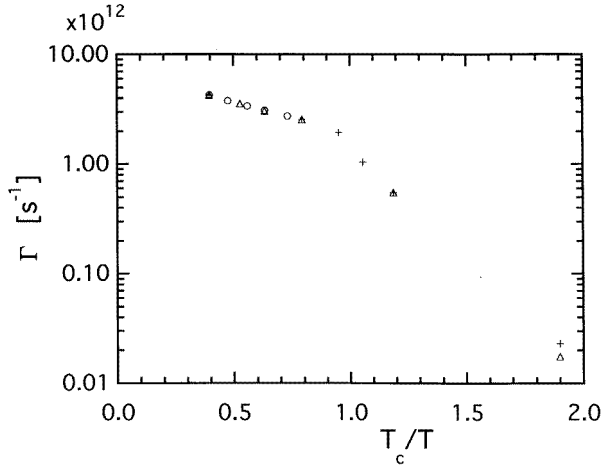

Figure 4. The temperature dependence of the jump rate, Γ. Calculated values are shown by crosses for $\beta/\beta_0 = 0$, triangles for $\beta/\beta_0 = 0.1$ and circles for $\beta/\beta_0 = 0.2$, respectively.

time evolution of $W(t)$ becomes similar to equation (13): the proton-transfer process can be regarded as a simple Markov process.

2.6. Incoherent neutron scattering functions

Direct experimental information on the proton transfer is obtained from incoherent neutron scattering. In this section, therefore, we calculate the scattering function [33] of incoherent neutron scattering defined by

$$S_{inc}(q, \omega) = \sum_i P_i \sum_f |M_{if}^{\alpha}|^2 \, \delta[\omega + (E_i - E_f)/\hbar] \tag{14}$$

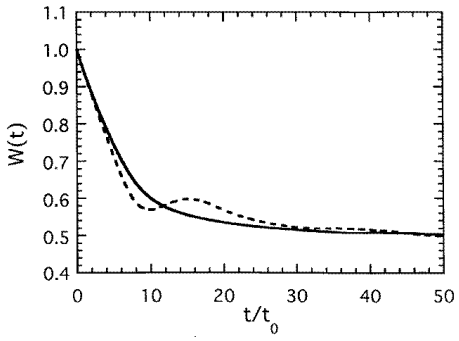

Figure 5. The time dependence of $W(t)$ at $T = 1.5T_c$. Results for $\beta/\beta_0 = 0$ and 0.2 are shown by the broken curve and the solid curve, respectively.

with

$$|M_{if}^{\alpha}|^2 = \sum_{\alpha} \langle i|e^{-i\boldsymbol{q}\cdot\boldsymbol{r}_\alpha}|f\rangle\langle f|e^{i\boldsymbol{q}\cdot\boldsymbol{r}_\alpha}|i\rangle \tag{15}$$

where $|i\rangle$ and $|f\rangle$, respectively, are the initial and final states of the system; P_i is the occupation probability of state i; $\boldsymbol{r}_\alpha$ is a position vector of proton α; and E_i and E_f, respectively, are energies of the initial and final states. Using the adiabatic approximation, $|M_{if}^{\alpha}|^2$ is rewritten as

$$|M_{if}^{\alpha}|^2 = \sum_{\alpha} \langle \chi_i|I_\alpha^*|\chi_f\rangle\langle \chi_f|I_\alpha|\chi_i\rangle \tag{16}$$

with

$$I_\alpha = \int \psi_\alpha^* e^{i\boldsymbol{q}\cdot\boldsymbol{u}_\alpha}\psi_\alpha \, d^3u_\alpha \tag{17}$$

where $|\chi_i\rangle$ ($|\chi_f\rangle$) is the initial (final) state of the dipole moments, ψ_α the ground-state wave function of proton α, and $\boldsymbol{u}_\alpha$ a position vector of the proton measured from the centre of the O–O bond connected by the proton.

According to I, we express ψ_α as the ground-state wave function of a harmonic oscillator in three dimensions:

$$\psi_\alpha = \psi_\alpha^x\psi_\alpha^y\psi_\alpha^z \tag{18}$$

with

$$\psi_\alpha^x = (m\omega_x/\pi\bar{h})^{1/4}\exp[-(m\omega_x/2\bar{h})(x_\alpha - x_\alpha^0)^2] \tag{19}$$

$$\psi_\alpha^y = (m\omega_y/\pi\bar{h})^{1/4}\exp[-(m\omega_y/2\bar{h})y_\alpha^2] \tag{20}$$

and

$$\psi_\alpha^z = (m\omega_z/\pi\bar{h})^{1/4}\exp[-(m\omega_z/2\bar{h})z_\alpha^2] \tag{21}$$

where ω_x, ω_x, and ω_z, respectively, are angular frequencies of the proton in the x, y and z directions. Here, we chose the direction of the O–O bond as the x axis, and assumed that the wave function has its maximum amplitude at $(x_\alpha^0, 0, 0)$. Using this wave function, we can express I_α as follows:

$$I_\alpha = \exp(-(\bar{h}/4m)[(\boldsymbol{q}\cdot\boldsymbol{x}_\alpha)^2/\omega_x + (\boldsymbol{q}\cdot\boldsymbol{y}_\alpha)^2/\omega_y + (\boldsymbol{q}\cdot\boldsymbol{z}_\alpha)^2/\omega_z])\exp(i(\boldsymbol{q}\cdot\boldsymbol{x}_\alpha)x_\alpha^0) \tag{22}$$

where $\boldsymbol{x}_\alpha$, $\boldsymbol{y}_\alpha$ and $\boldsymbol{z}_\alpha$ are unit vectors defined by

$$\boldsymbol{u}_\alpha = x_\alpha \boldsymbol{x}_\alpha + y_\alpha \boldsymbol{y}_\alpha + z_\alpha \boldsymbol{z}_\alpha \tag{23}$$

respectively.

In our model, both ω_x and x_α^0 depend strongly on a sum of dipole moments of two PO_4 tetrahedra connected by proton α, $\mu_i + \mu_j$, whereas dependencies of ω_y and ω_z on $\mu_i + \mu_j$ are weak. For simplicity, we assume that ω_y and ω_z are independent of $\mu_i + \mu_j$. In this approximation, $|M_{if}^\alpha|^2$ may be written as

$$|M_{if}^\alpha|^2 = \exp(-\eta_\alpha) G_{if}^\alpha \tag{24}$$

with

$$\eta_\alpha = (\hbar/2m)[(\boldsymbol{q}\cdot\boldsymbol{y}_\alpha)^2/\omega_y + (\boldsymbol{q}\cdot\boldsymbol{z}_\alpha)^2/\omega_z] \tag{25}$$

and

$$G_{if}^\alpha = \langle\chi_i|\mathrm{e}^{s_\alpha}|\chi_f\rangle\langle\chi_f|\mathrm{e}^{s_\alpha^*}|\chi_f\rangle \tag{26}$$

where s_α is defined by

$$s_\alpha = -\hbar(\boldsymbol{q}\cdot\boldsymbol{x}_\alpha)^2/4m\omega_x + \mathrm{i}(\boldsymbol{q}\cdot\boldsymbol{x}_\alpha)x_\alpha^o \tag{27}$$

and s_α^* is the complex conjugate of s_α.

By introducing Heisenberg operators defined by

$$s_\alpha(t) = \exp(\mathrm{i}H_{ad}t/\hbar)s_\alpha \exp(-\mathrm{i}H_{ad}t/\hbar) \tag{28}$$

the incoherent scattering function may be rewritten as follows:

$$S_{inc}(\boldsymbol{q},\omega) = \exp(-\eta_\alpha)G(\boldsymbol{q},\omega) \tag{29}$$

with

$$G(\boldsymbol{q},\omega) = \int \langle \mathrm{e}^{s_\alpha(t)}\mathrm{e}^{s_\alpha^*(0)}\rangle \mathrm{e}^{-\mathrm{i}\omega t}\,\mathrm{d}t \tag{30}$$

where $\langle\cdots\rangle$ means the thermal average, and H_{ad} is the Hamiltonian for the motion of dipole moments in the adiabatic approximation, defined by

$$H_{ad} = -\sum \frac{\hbar^2}{2M}\frac{\partial^2}{\partial\mu_i^2} + E_{pot}. \tag{31}$$

By using this expression, in principle we obtain the scattering function for protons under the adiabatic approximation. At present, however, it is difficult to perform the calculation directly.

We examine here the proton-transfer process in the temperature region where the motion of the system point is described classically. The scattering function in this temperature region may be estimated by regarding the operators $s_\alpha(t)$ and $s_\alpha^*(0)$ as c-numbers. Then equation (30) is rewritten as

$$G(\boldsymbol{q},\omega) = \int \langle \exp(s_\alpha(t) + s_\alpha^*(0))\rangle \mathrm{e}^{-\mathrm{i}\omega t}\,\mathrm{d}t \tag{32}$$

which is evaluated from the time evolution of dipole moments calculated in section 3.

To perform this calculation, knowledge about dependencies of ω_x and x_α^0 on $\mu_i + \mu_j$ is required. The frequency ω_x is obtained from the dependence on $\mu_i + \mu_j$ of the first excitation energy of protons along the direction of O–O bonds. For the potential parameters

we adopted, the dependence on $\mu_i + \mu_j$ of ω_x for a proton may be approximately expressed as

$$\hbar\omega_x = 0.095 \text{ eV} \qquad \text{for } 0 < |\mu_i + \mu_j|/2\mu_s < 0.26 \tag{33}$$

and

$$\hbar\omega_x = 0.078 + 0.085|\mu_i + \mu_j|/2\mu_s \text{ eV} \qquad \text{for } 0.26 \leqslant |\mu_i + \mu_j|/2\mu_s \tag{34}$$

respectively (see figure 2 in [18]).

For x_α^0, we assume the following relation:

$$x_\alpha^0/\Delta = (e^w - 1)/(e^w + 1) \tag{35}$$

where

$$w = \frac{\mu_i + \mu_j}{2\mu_s} z_c. \tag{36}$$

In figure 6 we show the dependence on ω of the incoherent scattering functions obtained by assuming $z_c = 2.5$ and $\Delta = 0.21$ Å. We note here that $|x_\alpha^0|$ for $|\mu_i + \mu_j|/2\mu_s = 1$ is 0.18 Å for these values of z_c and Δ, which is in good agreement with the position of a proton measured from the centre of an O–O bond, obtained from neutron diffraction measurements [22].

In the ferroelectric phase, there is a peak at about 30 meV (see figure 6(a)), whereas the peak disappears at high temperatures above T_c. The physical origin of the peak is the vibration motion of protons induced by electric dipole waves as discussed in I. Note that the value of the effective mass of dipole moments has been chosen so that a scattering peak caused by this mechanism appears at 30 meV.

In the paraelectric phase, there is no peak at near to 30 meV. For $\beta/\beta_0 = 0$, a peak appears at about 10 meV instead, as shown in figure 6(b). The height of this peak is at its maximum at $|q| \sim 8$ Å^{-1} and increases with increasing temperature. The appearance of this peak means that there is the vibration motion of protons with a period of about 3×10^{-13} s induced by thermal fluctuations in the paraelectric phase. This is consistent with the calculated result for $W(t)$ at $\beta/\beta_0 = 0$ described in section 3.

Table 2. Values of the fitting parameters, g, g_1, Ω, Ω_1 and ω_1, obtained by fitting equation (37) to the scattering function for $q = 8$ Å calculated for $T = 1.5T_c$. Here, an arbitrary unit is used for g and g_1.

β/β_0	g	g_1	$\hbar\Omega$ (meV)	$\hbar\Omega_1$ (meV)	$\hbar\omega_1$ (meV)
0.0	9.3	5.2	2.3	4.5	10.8
0.1	13.7	2.9	4.2	4.7	9.9
0.2	14.6	2.5	4.2	5.6	8.4

To perform more quantitative analysis of the scattering function in the paraelectric phase, we assume that the scattering function can be expressed as a sum of two Lorentzian distributions:

$$G_\alpha(\omega) = g\frac{\Omega}{(\omega^2 + \Omega^2)} + g_1\frac{\Omega_1}{((\omega - \omega_1)^2 + \Omega_1^2)}. \tag{37}$$

For various values of β, calculated scattering functions are fairly well reproduced by the best-fit curve obtained from this expression by adjusting five parameters, g, Ω, g_1, Ω_1 and ω_1. In table 2, the five parameters obtained are listed for $T = 1.5T_c$. Note here

(*a*)

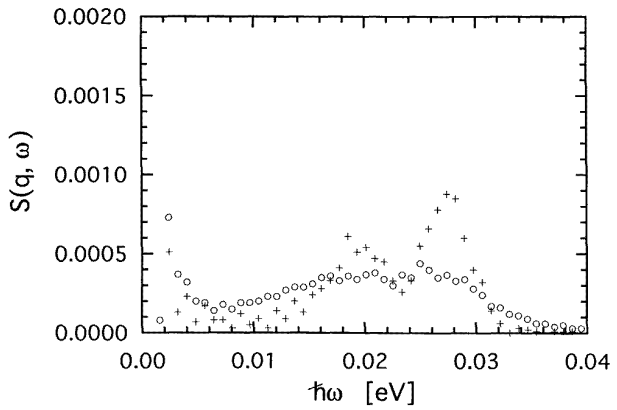

(*b*)

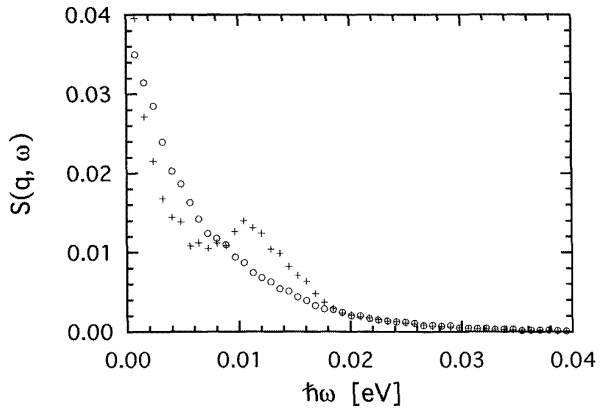

Figure 6. The dependence on ω of the incoherent scattering functions for (a) $T = 0.5T_c$, and (b) $T = 1.5T_c$. Results for $\beta/\beta_0 = 0$ and 0.2 are shown by crosses and circles, respectively. For scattering vectors, $\boldsymbol{q}$, it is assumed that $|\boldsymbol{q}| = 8$ Å^{-1} and its direction is parallel to the a axis of a KDP crystal.

that $g_1/g = 0.15$ at $\beta/\beta_0 = 0.2$. This means that, in this case, the scattering function is substantially regarded as a simple Lorentzian distribution with its maximum at $\omega = 0$—that is, a quasi-elastic scattering peak with a broad width.

In figure 7 we shown the temperature dependence of Ω obtained by fitting equation (37) to the scattering function calculated for $\beta/\beta_0 = 0.2$.

We note here that the features of the scattering function obtained do not depend on details of the dependence on $\mu_i + \mu_j$ of ω_x and x_α^0.

3. Discussions

Recently, in the paraelectric phase of KDP, a strong quasi-elastic peak was found in the energy spectrum of incoherent neutron scattering measured by Ikeda *et al* [15]. This peak extended over a wide range of the energy transfer reaching to 20 meV and its line shape was

expressed in terms of the Lorentzian distribution. This result was interpreted as suggesting that there is a stochastic proton-transfer process in which a proton jumps between the two stable positions separated by about 0.32 Å at a jump rate of the order of 10^{12} s^{-1}.

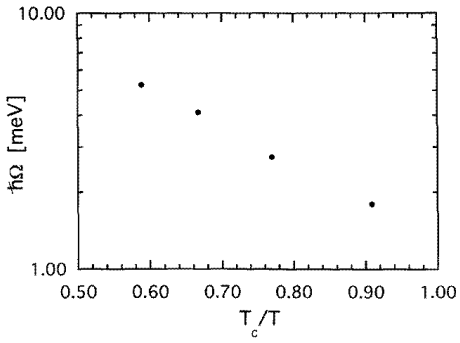

Figure 7. The temperature dependence of Ω determined from the calculated result for scattering functions for $\beta/\beta_0 = 0.2$ in the paraelectric phase. For scattering vectors, $\boldsymbol{q}$, it is assumed that $|\boldsymbol{q}| = 8$ Å^{-1} and its direction is parallel to the a axis of a KDP crystal.

Yamada and Ikeda [34] regarded KDP as a proton–phonon system and tried to analyse the temperature dependence of the widths of the observed quasi-elastic peaks under the assumption that the hopping rate is expressed by

$$\Gamma = (\pi/4\hbar^2 E_a kT)^{1/2}|J|^2 \mathrm{e}^{-E_a/kT} \tag{38}$$

as given by Flynn and Stoneham [30]. The result was that the parameter values must be chosen as $E_a = 37$ meV and $J = 66$ meV to reproduce the temperature dependence of the peak width of the quasi-elastic peak.

Since equation (38) has been derived in the non-adiabatic limit, the criterion for the non-adiabatic transition to occur, that is, $J \ll \hbar\omega_d$, must be satisfied as mentioned in section 2. Accordingly, this value of J means that phonons with very large energy ($\gg$66 meV) coupling with the motion of protons must exist in KDP. At present, however, evidence that such phonons exist has not been obtained. In addition, the value of J is too large because the tunnelling-spilt energy ($2J$) becomes of the same order as the excitation energies of protons observed via incoherent neutron scattering. These facts suggest that a process due to the tunnelling effect of a proton at the saddle-point configuration is not regarded as the mechanism of the proton transfer in KDP, and, accordingly, that the proton transfer in KDP is due to the adiabatic transition, but not the non-adiabatic transition.

In the present calculation assuming the adiabatic transition, we found that a proton in the paraelectric phase moves between two sites at a rate comparable to a frequency of the vibration motion of the system point, as expected. We also found that the proton motion for $\beta/\beta_0 = 0$ is not regarded as a simple Markov process since the time dependence of the proton position has a component changing periodically. The existence of this component means that an inelastic scattering peak appears in the energy spectrum. In fact, it was shown by our calculation of the scattering function that an inelastic scattering peak appears when the random force is small.

When the random force is large, on the other hand, a quasi-elastic peak becomes dominant instead of this inelastic scattering peak. This means that a quasi-elastic peak is observed in the energy spectrum of neutron scattering for a system with a large value of β. KDP seems to be regarded as such a system. Thus we conclude that our model gives a

qualitative explanation for the observation of the quasi-elastic scattering peak by Ikeda *et al* [15].

Quantitatively, however, observed widths of the quasi-elastic peak are greater than the calculated ones by a factor of about 4 since, for example, an observed value of the width is 7 meV at $T = 130$ K [15]. This difference disappears if we choose the effective mass, M, as a twelfth the present value. In this case, however, a peak due to the vibration motion of protons induced by dipole waves must be observed at near to 120 meV in the ferroelectric phase. There is no observation of such a peak. Accordingly, the validity of such a choice of M is questionable. At present, therefore, the origin of this disagreement is not clear.

In judging the reliability of our model for the proton transfer, it is important to recall that, in our model, the jump rate is completely determined by the motion of dipole moments. The present result, that the proton transfer occurs at a rate of 10^{12} s^{-1}, implies that the relaxation process of the dipole moment has a relaxation rate of the order of 10^{12} s^{-1}. Such relaxation motion of the dipole moment is expected to be obtained from measurements of the dielectric dispersion. In fact, Horioka *et al* [35] observed the dielectric constant in KDP and found that, in the paraelectric phase, a dipole moment has a relaxation time of about 10^{-13} s. Although it is not clear whether or not the relaxation observed by them can be ascribed to the motion of the dipole moment induced by the deformation of PO_4 tetrahedra, this observation seems to indicate the applicability of our model for the proton transfer in KDP. More detailed calculations on the relaxation process of dipole moments will be reported in forthcoming publications, based on the present approach.

Concerning the relaxation of dipole moments, Matsumoto and Ogura [36] have revealed the conclusion that there is a relaxation process with a relaxation rate of the order of 10^{12} s^{-1}, on the basis of the Slater–Takagi model modified by Silsbee *et al* [37]. In their calculation, however, the transition probability per unit time from proton configuration i to j, W_{ij}, is assumed as

$$W_{i,j} = (kT/2\pi\bar{h}) \exp(-E_{ij}/kT)$$

where E_{ij} is an energy difference between configurations i and j. Since the proton configurations that are taken into account in the Slater–Takagi model are stable configurations, but not saddle-point configurations, their treatment seems to be inadequate for estimating the magnitude of the relaxation time of dipole moments. We emphasize here that our model gives a qualitative explanation for both experiments—namely, the inelastic neutron scattering in the low-energy region and the measurement of the dielectric dispersion, as described above.

We note that, for $K_3H(SO_4)_2$ and $Rb_3H(SO_4)_2$, a peak at about 5 meV has been found in the energy spectra measured by using incoherent neutron scattering [38]. As shown in our calculation, observation of such low-energy excitations is possible in a hydrogen-bonded material in which the effect of the random force is small. The origin of the low-energy excitations observed might, therefore, be ascribed to the proton transfer in a system with small β. To confirm this inference, however, it is necessary to perform more detailed calculations taking account of the crystal structure.

Finally, we make some remarks as to the validity of the present calculations. Our calculations were performed in the framework of the classical approximation for the motion of dipole moments. The conclusion obtained here is, therefore, justified only when this approximation is valid. It is clear that the approximation is inadequate at low temperatures. In fact, the height of the peak at about 30 meV in the ferroelectric phase rapidly increased with increasing temperature in the present calculations. This temperature dependence clearly differs from the one obtained in I: in the quantum mechanical treatment, the height of the

peak increases little with increasing temperature, in agreement with observation.

A criterion for the validity of the classical approximation is that the thermal energy is larger than the vibration energy of relevant modes. For the peak at 30 meV described above, this criterion is not satisfied since, in the ferroelectric phase, the thermal energy kT is sufficiently smaller than 30 meV. Accordingly, the classical approximation is inadequate for this mode.

For the peak at 10 meV in the paraelectric phase, however, it holds that $kT \geqslant 10$ meV. Accordingly, we believe that the calculation method adopted here is not a poor approximation for the proton transfer in the ferroelectric phase, and accordingly the present calculation is sufficiently good to allow us to conclude that it indicates the existence of a proton-transfer process with a very fast jump rate.

4. Conclusion

From the examination of our model proposed to explain the ferroelectric phase transition, we conclude that, in the paraelectric phase, the mechanism of proton transfer in KDP is the adiabatic transition and its jump frequency is of the order of 10^{12} s^{-1}.

References

[1] Kobayashi K K 1968 *J. Phys. Soc. Japan* **24** 497
[2] Yoshimitsu K and Matsubara T 1968 *Prog. Theor. Phys. Suppl. (Kyoto)* 109
[3] Cochran W 1969 *Adv. Phys.* **18** 157
[4] Tokunaga M 1970 *Ferroelectrics* **1** 195
[5] Matsushita E and Matsubara T 1982 *Prog. Theor. Phys.* **67** 1
[6] Matsubara T and Matsushita E 1984 *Prog. Theor. Phys.* **71** 209
[7] Slater J C 1941 *J. Chem. Phys.* **9** 16
[8] Takagi U 1948 *J. Phys. Soc. Japan* **3** 271
[9] Noda Y and Kasatani H 1991 *J. Phys. Soc. Japan* **60** 13
[10] Noda Y, Watanabe Y, Kasatani H, Terauchi H and Gesi K 1991 *J. Phys. Soc. Japan* **60** 1972
[11] Kojyo N and Onodera Y 1988 *J. Phys. Soc. Japan* **57** 4391
[12] Blinc R 1960 *J. Phys. Chem. Solids* **13** 204
[13] Tokunaga M and Matsubara T 1966 *Prog. Theor. Phys.* **35** 581
[14] Tominaga Y, Kasahara M, Urabe H and Tatsuzaki I 1983 Solid *State Commun.* **47** 835
[15] Ikeda S, Noda Y, Sugimoto H and Yamada Y 1994 *J. Phys. Soc. Japan* **63** 1001
[16] Ichikawa M 1981 *Chem. Phys. Lett.* **79** 583
[17] Nelmes R J 1988 *J. Phys. C: Solid State Phys.* **21** L881
[18] Sugimoto H and Ikeda S 1991 *Phys. Rev. Lett.* **67** 1306
[19] Sugimoto H and Ikeda S 1993 *J. Phys.: Condens. Matter* **5** 7409
[20] Samara G A 1973 *Ferroelectrics* **5** 25
[21] Tominaga Y, Urabe H and Tokunaga M 1983 *Solid State Commun.* **48** 265
[22] Tun T, Nelmes R J, Kuhs W F and Stanfield R F D 1988 *J. Phys. C: Solid State Phys.* **21** 245
[23] Shibata K and Ikeda S 1992 *J. Phys. Soc. Japan* **61** 411
[24] Sugimoto H and Ikeda S 1994 *J. Phys.: Condens. Matter* **6** 5561
[25] Landau L 1932 *Z. Phys. Sowjet.* **1** 88; 1932 *Z. Phys. Sowjet.* **2** 46
[26] Zener C 1932 *Proc. R. Soc.* A **137** 696; 1933 *Proc. R. Soc.* A **140** 660
[27] Holstein T 1978 *Phil. Mag.* **37** 49
[28] Fukai Y and Sugimoto H 1985 *Adv. Phys.* **34** 263
[29] Holstein T 1959 *Ann. Phys., NY* **8** 325, 343
[30] Flynn C P and Stoneham A M 1970 *Phys. Rev.* B **1** 3966
[31] See, e.g.,
Geisel T 1979 *Physics of Superionic Conductors* ed M B Salamon (Berlin: Springer)
[32] See, e.g.,
Heermann D W1990 *Computer Simulation Methods in Theoretical Physics* 2nd edn (Berlin: Springer)

[33] See, e.g.,
Callaway J 1991 *Quantum Theory of the Solid State* 2nd edn (San Diego, CA: Academic)
[34] Yamada Y and Ikeda S 1994 *J. Phys. Soc. Japan* **63** 2691
[35] Horioka M, Nakagawa T, Ota J and Abe R 1996 to be published
[36] Matsumoto Y and Ogura K 1993 *J. Phys. Soc. Japan* **62** 3519
[37] Silsbee H B, Uehling E A and Schmit V H 1964 *Phys. Rev.* **133** A165
[38] Fillaux F and Lautie A 1991 *Chem. Phys.* **154** 4201